nature climate change

ARTICLES

https://doi.org/10.1038/s41558-020-0776-2

Check for updates

# Decreased motility of flagellated microalgae long-term acclimated to $CO_2$-induced acidified waters

Yitao Wang[1,2], Xiao Fan[1], Guang Gao[3], John Beardall[3,4], Kazuo Inaba[5], Jason M. Hall-Spencer[5,6], Dong Xu[1], Xiaowen Zhang[1], Wentao Han[1], Andrew McMinn[7] and Naihao Ye[1,2] ✉

**Motility plays a critical role in algal survival and reproduction, with implications for aquatic ecosystem stability. However, the effect of elevated $CO_2$ on marine, brackish and freshwater algal motility is unclear. Here we show, using laboratory microscale and field mesoscale experiments, that three typical phytoplankton species had decreased motility with increased $CO_2$. Polar marine *Microglena* sp., euryhaline *Dunaliella salina* and freshwater *Chlamydomonas reinhardtii* were grown under different $CO_2$ concentrations for 5 years. Long-term acclimated *Microglena* sp. showed substantially decreased photo-responses in all treatments, with a photophobic reaction affecting intracellular calcium concentration. Genes regulating flagellar movement were significantly downregulated ($P < 0.05$), alongside a significant increase in gene expression for flagellar shedding ($P < 0.05$). *D. salina* and *C. reinhardtii* showed similar results, suggesting that motility changes are common across flagellated species. As the flagella structure and bending mechanism are conserved from unicellular organisms to vertebrates, these results suggest that increasing surface water $CO_2$ concentrations may affect flagellated cells from algae to fish.**

Marine phytoplankton account for nearly 50% of annual global primary productivity[1]. They are the basis of most marine food webs and provide materials and energy to support complex and productive higher trophic levels[2]. Many phytoplankton migrate vertically on a daily basis to optimize photosynthesis and decrease predation[3]. For many algae, this motion is achieved by the beating of flagella[4]. Unicellular flagellate algae swim towards light by positive phototaxis but if the light is too strong they use photophobic reaction responses to swim away and avoid damage (negative phototaxis)[5,6].

Here, we assess the effects of rising $CO_2$ levels on movement in a range of algae. About one-third of $CO_2$ released into the atmosphere as a result of human activity has been taken up by surface water masses since the Industrial Revolution, with potential effects on flagellated marine biota. When $CO_2$ dissolves in water it lowers the pH, potentially affecting the motility of algae[7–9]. Lowered pH alters the vertical migration and distribution of *Heterosigma akashiwo*[10] but the effects of $CO_2$-induced acidification on algal motility are rarely reported, particularly after long-term acclimation.

In our study, three flagellated microalgae, representing different taxa and originating from different aquatic environments (marine/sea ice habitat, estuarine and freshwater)—*Microglena* sp. from the Antarctic, the widely distributed euryhalophyte *Dunaliella salina* and the freshwater model microalga *Chlamydomonas reinhardtii*—were investigated. We studied changes in cell motility, as measured by positive and negative phototaxis and responses, at different $CO_2$ concentrations, including pre-industrial levels, and linked this to gene-expression patterns. *Microglena* sp. was cultured at 280, 400, 700, 1,000, 1500 and 2,000 ppm $CO_2$ for 5 yr and, over the same period, *C. reinhardtii* and *D. salina* were cultured at 400, 1,000 and 2,000 ppm. In these experiments, we measured both average and instantaneous velocities, representing the ability of microalgae to search for optimal light intensity and quickly escape predators, respectively. We also carried out a field experiment on *Microglena* sp. using natural sunlight to induce positive/negative phototaxis. We address two questions: first, what is the effect of elevated $CO_2$ on microalgal motility? Second, what are the molecular mechanisms that underpin photoreception and motility at the transcriptome level in response to elevated $CO_2$? We sequenced the entire genome of *Microglena* sp. and provide results from this marine species here. Our parallel experiments on the brackish water and freshwater flagellates showed the same responses.

As $CO_2$ levels increased, the average velocity of *Microglena* sp., *C. reinhardtii* and *D. salina* decreased; all the differences were significant at 1,000 ppm ($P < 0.05$, Fig. 1a–d and Extended Data Fig. 1). Further verification experiments using natural sunlight showed that the velocity of the algal cells decreased under acidification and that the decrease was also significant at 1,000 ppm ($P < 0.05$, Fig. 1e–h). As shown in Supplementary Figs. 1–3, the higher the velocity of the cells, the higher proportion of cell numbers in the movement direction. These results were consistent with the results that are shown in Fig. 1 and Extended Data Fig. 1. Measurements of instantaneous velocities showed similar results to those of average velocities (Extended Data Figs. 2–4). Real-time fluorescence images of the cells reflected the changes in cell velocity under different values for partial pressure of $CO_2$ ($p_{CO_2}$) (Supplementary Fig. 4). Elevated $p_{CO_2}$ had an adverse effect on cell motility (Supplementary Fig. 4). Furthermore, the differential roles of seawater $p_{CO_2}$ and pH

[1]Yellow Sea Fisheries Research Institute, Chinese Academy of Fishery Sciences, Qingdao, China. [2]Function Laboratory for Marine Fisheries Science and Food Production Processes, Qingdao National Laboratory for Marine Science and Technology, Qingdao, China. [3]State Key Laboratory of Marine Environmental Science & College of Ocean and Earth Sciences, Xiamen University, Xiamen, China. [4]School of Biological Sciences, Monash University, Clayton, Victoria, Australia. [5]Shimoda Marine Research Center, University of Tsukuba, Shizuoka, Japan. [6]School of Biological and Marine Sciences, University of Plymouth, Plymouth, UK. [7]Institute of Antarctic and Southern Ocean Studies, University of Tasmania, Tasmania, Australia. ✉e-mail: yenh@ysfri.ac.cn

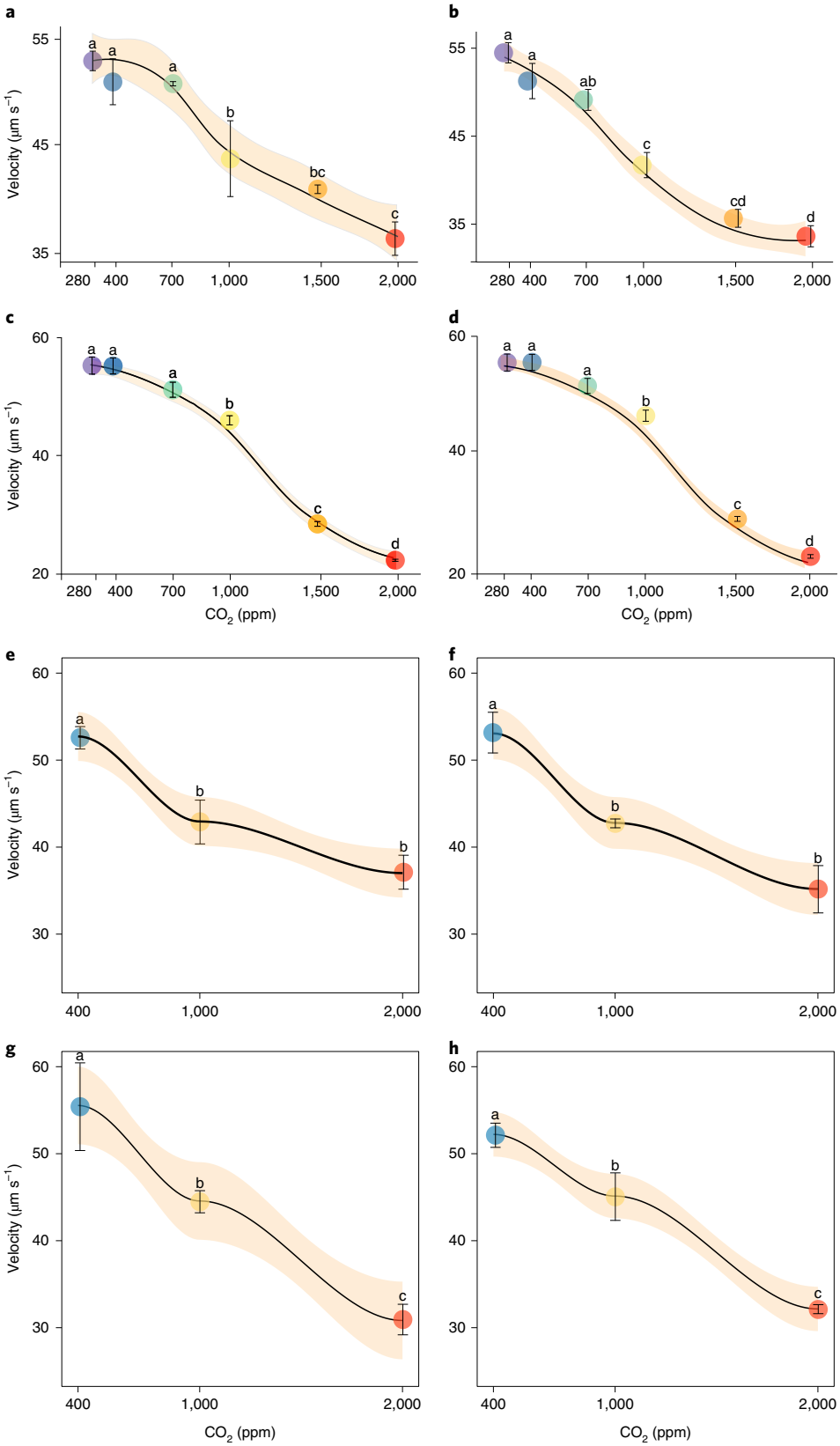


**Fig. 1 | Average velocity of *Microglena* sp. induced by artificial light and sunlight in the field. a–d**, Phototaxis induced by white light: positive phototaxis in the vertical direction (**a**); negative phototaxis in the vertical direction (**b**); positive phototaxis in the horizontal direction (**c**); negative phototaxis in the horizontal direction (**d**). **e–h**, Phototaxis induced by sunlight: positive phototaxis in the vertical direction (**e**); negative phototaxis in the vertical direction (**f**); positive phototaxis in the horizontal direction (**g**); negative phototaxis in the horizontal direction (**h**). Curve fitting was performed by a 'loose' method using a geometric smoothing function in the R package ggplot2. The shaded part represents the 95% confidence interval of the fitted curve. Mean ± s.d. values per experimental assay are given ($n = 3$). Different letters (a–d) in each panel indicate significant differences ($P < 0.05$) among treatments.

on cell motion were studied. The results showed that the decrease of pH resulted in a significant decrease of cell velocity ($P<0.05$, Supplementary Figs. 5a–d, 6a–d and 7a–d) but the increase of $CO_2$ without a pH shift had no significant effect ($P>0.05$, Supplementary Figs. 5e–h, 6e–h and 7e–h).

In the study of positive/negative phototaxis under various $CO_2$ treatments and different experimental scales, we found that the average velocity of *Microglena* sp., *C. reinhardtii* and *D. salina* showed no significant difference between laboratory microscale and field mesoscale experiments ($P>0.05$, Supplementary Tables 1–5); except for movement of *Microglena* sp. in the vertical direction under 1,500 and 2,000 ppm $CO_2$ (Supplementary Table 1), wherein the velocity of positive phototaxis was significantly higher than the velocity of negative phototaxis ($P<0.05$). This may be due to buoyancy induced by $O_2$ released by photosynthesis, as our vertical phototaxis response direction was designed to be bottom-up (Supplementary Figs. 8a, 9a and 10a).

The effect of positive/negative phototaxis on instantaneous velocity was striking. The positive phototaxis velocity of *Microglena* sp. was significantly higher than that of the negative phototaxis velocity in the both vertical and horizontal directions, except for the horizontal motion under 400 ppm $CO_2$ ($P<0.05$, Supplementary Table 6). The positive phototaxis velocities of *C. reinhardtii* and *D. salina* were also significantly higher than those of the negative phototaxis velocities in the horizontal direction ($P<0.05$), a result that was similar to that of *Microglena* sp. However, in the vertical direction, the negative phototaxis velocities of *C. reinhardtii* and *D. salina* were significantly higher than those of the positive phototaxis velocities ($P<0.05$), except for the 2,000-ppm treatment of *C. reinhardtii* in the vertical direction (Supplementary Tables 7 and 8).

Our study shows that elevated $CO_2$ significantly reduced the instantaneous velocity and average velocity of the cells at both laboratory microscale and field mesoscale levels in *Microglena* sp., *C. reinhardtii* and *D. salina* ($P<0.05$, Fig. 1 and Extended Data Figs. 1 and 2–4). We carried out the analyses of algal photoresponse under blue light but the results were the same using white light or sunlight (Supplementary Figs. 11 and 12 and Supplementary Tables 9–12).

There was a substantially increase in deflagellation and a decrease in restoration of motility under $CO_2$-induced acidification (Fig. 2). Long-term $CO_2$ treatments led to an increase in the deflagellation ratio, resulting in a decrease in the number of motile cells (Fig. 2a). Increased $CO_2$ prolonged the recovery time of the proportion of motile cells (Fig. 2b). When $CO_2$ levels exceeded 1,000 ppm, the recovery time of *Microglena* sp. motility was >3 h, significantly longer than under levels of 400 ppm ($P<0.05$, Fig. 2b–d). This may be related to pH-shock, in which lowering pH induces $Ca^{2+}$-influx and deflagellation[11]. Non-motile cells without flagella usually sink to the bottom and die under natural conditions[4,12]. Although *Microglena* sp., *C. reinhardtii* and *D. salina* growth increased with acidification in laboratory conditions (Supplementary Figs. 13 and 14), decreased motility (Fig. 1 and Extended Data Fig. 1) would probably prove fatal in the natural environment due to a decreased capacity to escape from biotic and abiotic threats. Thus, we predict that under natural conditions, elevated $CO_2$ will adversely affect the survival of microalgae with flagella.

To clarify the impact of increased $CO_2$ on flagella, the molecular mechanism by which acidification causes a decrease in swimming velocity was studied in *Microglena* sp. (Fig. 3). We focused on 12 flagella bending genes (Supplementary Table 13) that showed changes in gene expression from transcriptome data and were verified by polymerase chain reaction with reverse transcription (RT–PCR). Under long-term acidification, transcriptome data showed that genes of *Microglena* sp. that are involved in the initial step for $Ca^{2+}$-signalling were all downregulated ($P<0.05$, Fig. 3f). Genes that promote flagellar motion were all downregulated in the 1,000-ppm $CO_2$ treatments compared to those in the 400-ppm treatment ($P<0.05$, Fig. 3d,e). However, CK1 and PKA, which suppress flagellar motion, were significantly upregulated ($P<0.05$, Fig. 3e). Furthermore, dynein assembly genes, DNAAF3/PF22, were downregulated and deflagellation genes, DIP13/NA14, were upregulated ($P<0.05$, Fig. 3c). DC3, a $Ca^{2+}$-binding component of the dynein-docking complex involved in the dynein assembly, was highly upregulated ($P<0.05$, Fig. 3d). The changes in gene-expression pattern in *Microglena* sp. caused by acidification were not restricted to motility genes but occurred at the whole genome level (Supplementary Fig. 15). Real-time imaging showed that intracellular $Ca^{2+}$ concentration during positive phototaxis increased, whereas it decreased during negative phototaxis, when the cells were acclimatized to high $CO_2$ (Fig. 3g and Supplementary Fig. 16). These changes were also observed in *C. reinhardtii* and *D. salina* (Supplementary Fig. 17).

Given the 5-yr length of our experiment, we queried whether genetic modifications had occurred in the genome of *Microglena* sp. It was shown that the overall numbers of single nucleotide polymorphism (SNP) sites were evenly distributed across the genome with a few peaks at specific sites (Supplementary Fig. 18). The normal sample (control, sampling 5 yr ago) was significantly lower in overall SNPs number compared with the samples under the 5-yr experiment (400, 1,000 and 2,000 ppm) ($P<0.05$, Supplementary Fig. 19). In addition, in all samples under the 5-yr treatment, the number of overall SNP sites increased as the $CO_2$ concentration went up (Supplementary Fig. 19), indicating that acidification was strongly affecting the genetic modifications. Focusing on the relationship between genetic modification and flagellum movement, we specifically studied the SNP profiles of 14 genes that are directly related to motility. It can be seen from Supplementary Fig. 20 that the accumulation of single nucleotide mutations in all the motion-related genes is positively correlated with the degree of acidification ($R^2>>0$). The correlation is significant for six of the 14 genes ($P<0.05$, *F*-statistic, Lm method in R). These genes play a role in motility, phosphorylation and dynein assembly, indicating genetic adaptation of motility to oceanic acidification. To investigate the effect of genetic mutations on codons, we calculated the synonymous mutation rate ($K_s$) and the non-synonymous ($K_a$) mutation rate of motion-related genes (Supplementary Fig. 21). We found that $K_a$ was generally less than $K_s$ for 400 ppm ($P<0.05$) $CO_2$, indicating that the presence of more mutations did not cause changes in the coding protein under 400 ppm treatment for 5 yr. However, the difference did not exist for 1,000 and 2,000 ppm $CO_2$. This indicates that with the increase of acidification gradient, more non-synonymous mutations occurred, thus accelerating the selection effect of environment on individual genes. This conjecture is supported somewhat by $K_a/K_s$. We found that the median value of $K_a/K_s$ climbed as acidification increased, although changes were not statistically significant ($P>0.05$).

The phototactic pathway of *Microglena* sp. is not fully understood. Due to the highly conserved structure of the flagellum and similarity of photosensitive organs in flagellated green microalgae, *C. reinhardtii* was used to annotate flagellate-related genes in the *Microglena* sp. motility-related genes, so the existing *C. reinhardtii* pathway was used to study the *Microglena* sp. motility-related genes. The phototactic pathway of *Chlamydomonas* primarily consists of three steps: (1) a light inward current in the eyespot, which functions as a light reflector and light-gated ion channel[11]; (2) a photocurrent depolarized activated voltage-gated $Ca^{2+}$ channel in flagella[5,11,13]; and (3) flagellar bending stimulated by $Ca^{2+}$ and inhibited by cAMP[5]. Flagellar beat is driven by the axonemal dyneins, which are regulated by $Ca^{2+}$-binding proteins LC4, DC3 (ref. [11]) and a phosphorylation protein IC138. The components of radial spokes and central pair apparatus also play a major role in regulating axonemal

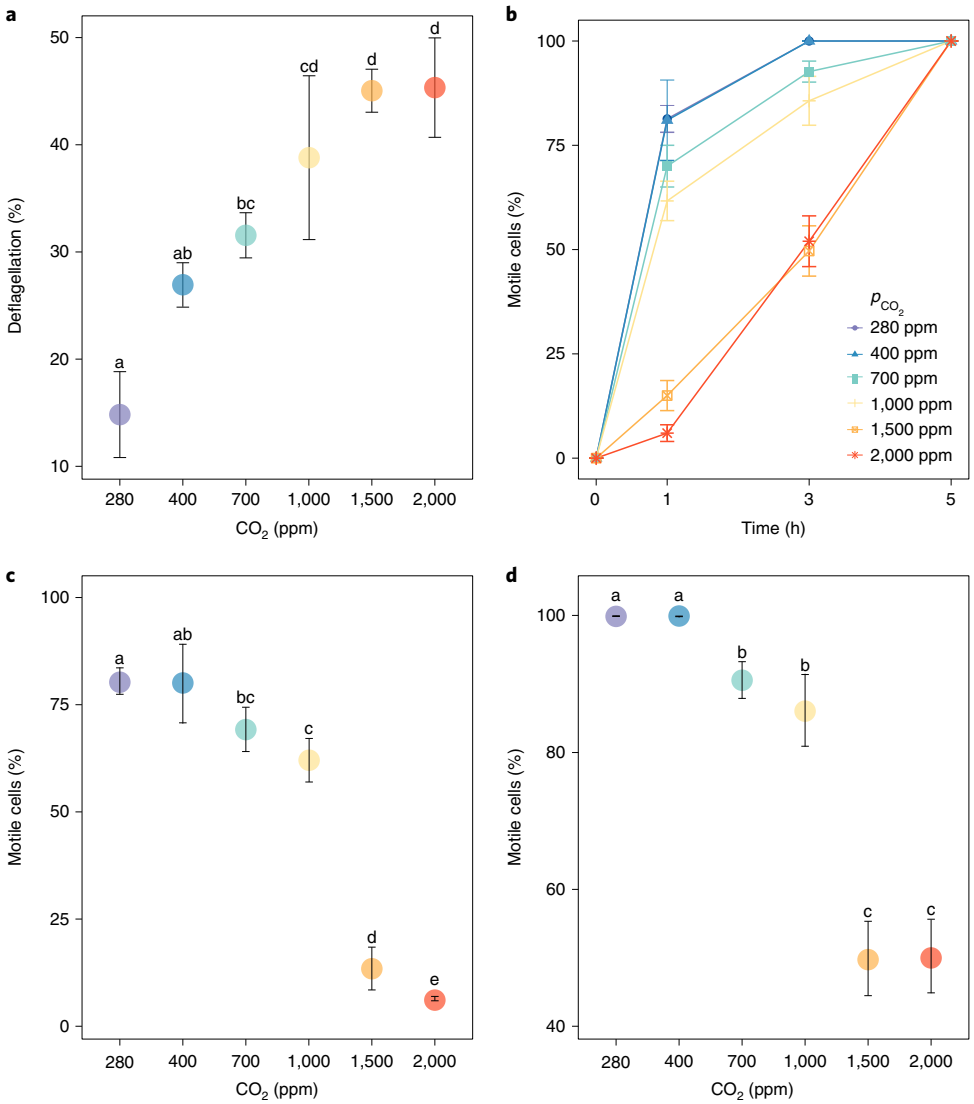


**Fig. 2 | $CO_2$ concentration effects on proportion of *Microglena* sp. showing deflagellation and restoration of motility. a**, Deflagellation percentage. **b**–**d**, Percentage of motile cells (**b**); after 1 h (**c**); after 3 h (**d**). Mean ± s.d. values per experimental assay are given ($n = 3$). Different letters (a–e) in each panel indicate significant differences ($P < 0.05$) among treatments.

dyneins[5,11,13–15]. The present study shows that long-term acidification negatively affected expression of genes related to photosensitivity, signal transduction and the regulation of dyneins and flagellar motility (Fig. 3). In addition, the acidification resulted in decreased formation and stability of flagella (Fig. 3c). Taken together, these results suggest that long-term exposure to acidification has negative effects on the motility of *Microglena* sp. Under the strongest emissions scenario, Antarctic terrestrial ice-free areas could increase by close to 25% by the end of the century, causing fundamental changes to the region[16]. Changes in phytoplankton species composition and the seasonality of production affect Antarctic food webs and are induced by the retreat of winter sea ice[17]. As a polar alga, *Microglena* sp. will be affected by both sea ice loss and acidification, since its light compensation point is reduced under ocean acidification (Fig. 4a).

*Microglena* sp. survives under sea ice all year round[18]. Due to the strong attenuation of natural light through the ice, light intensity under the ice is much lower than in non-ice-covered waters[9] and *Microglena* sp. is well adapted to an under-ice, low-light environment[18]. When sea ice melts, accelerated by climate change, *Microglena* sp. is exposed to much greater light intensities. Consequently, the vertical migration distance increases if cells are to position themselves in a region of appropriate light intensity (Fig. 4). As shown in Fig. 4c, we calculated how much time it would take *Microglena* sp. to cover the daily vertical migration (DVM, the vertical distance between the water layer that corresponds to the light compensation point for photosynthesis of algae and the water layer that corresponds to the light saturation point for photosynthesis of algae) using the average and instantaneous velocities under positive/negative phototactic responses. Under positive phototaxis, at 2,000 ppm, the average velocity is 0.13 m $h^{-1}$ and the instantaneous velocity is 0.29 m $h^{-1}$. It would take *Microglena* sp. 2.57–5.65 d to cross the DVM. For *Microglena* sp. adapted to 280 ppm $CO_2$, it would take 14.64 h to 1.89 d. It also takes an extended period of time to cross the DVM under increased $CO_2$ during the negative phototaxis response. However, an increase in ocean acidification will decrease the motility of *Microglena* sp., which we suspect will put this organism at a disadvantage such that it will probably

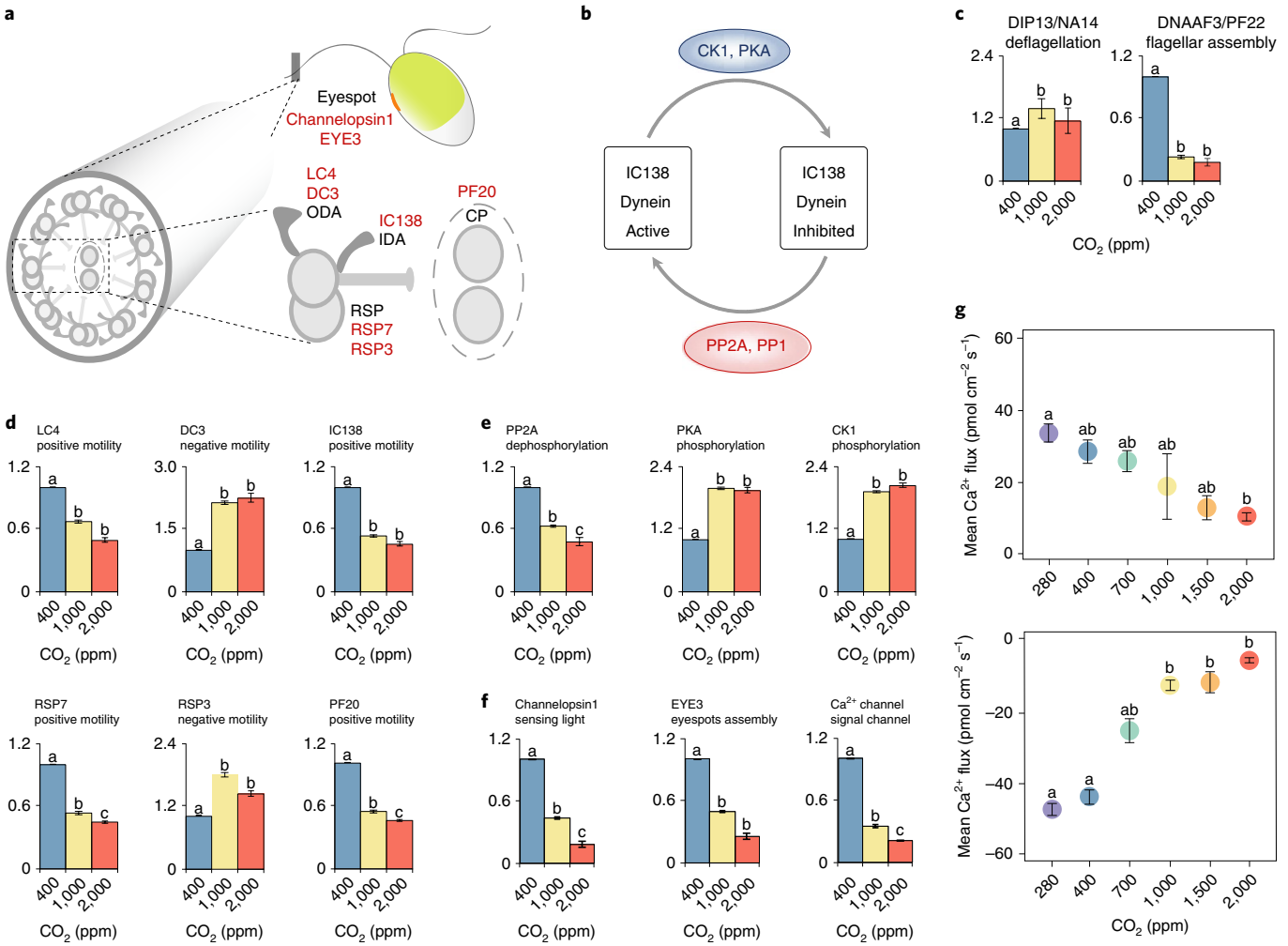


**Fig. 3 | Changes in the expression of motility-related genes. a**, Schematic diagram of light sensation and $Ca^{2+}$-mediated flagellar beating in *Microglena* sp. ODA, outer dynein arm; IDA, inner dynein arm; RSP, radial spoke protein; CP, central pair apparatus. The genes for RT–PCR are listed in red. **b**, Regulation of an inner dynein arm by the phosphorylation/dephosphorylation of IC138 via protein kinases and phosphatases. **c**, Changes of gene expression for deflagellation and flagellar assembly under the 1,000 and 2,000 ppm treatments relative to the 400 ppm treatment. **d**, Changes of gene expression for dynein subunits under the 1,000 and 2,000 ppm treatments relative to the 400 ppm treatment. **e**, Changes of gene expression for the regulation of IC138 under the 1,000 and 2,000 ppm treatments relative to the 400 ppm treatment. **f**, Changes of gene expression for eyespot and $Ca^{2+}$ regulation under the 1,000 and 2,000 ppm treatments relative to the 400 ppm treatment. **g**, The mean flux of $Ca^{2+}$ under different $p_{CO_2}$ scenarios. Mean ± s.d. values per experimental assay are given ($n = 3$). Upper, $Ca^{2+}$ efflux under positive phototaxis. Lower, $Ca^{2+}$ influx under negative phototaxis. '−' on the vertical scale means $Ca^{2+}$ entry. LC4, flagellar outer dynein arm light chain 4; DC3, outer dynein arm docking complex protein 3; IC138, a 138 kDa intermediate chain of I1/f inner arm dynein; RSP, radial spoke protein; PF20, a protein of the central pair apparatus; PKA, cAMP-dependent protein kinase; PP2A, protein phosphatase 2A; CK1, casein kinase 1; DIP13/NA14, deflagellation inducible protein; DNAAF3/PF22, axonemal dynein assembly factor. Mean ± s.d. values per experimental assay are given ($n = 3$). Different letters (a–c) in each panel indicate significant differences ($P < 0.05$) among treatments.

be outcompeted in ice-free conditions, changing the Antarctic ecosystem. *C. reinhardtii* and *D. salina*, which are not protected by ice, experience dramatic changes in the light in their environment. In this case, the cells can escape light stress through motility. Prolonged exposure to bright light increases the risk of light damage and increasing $CO_2$ concentrations decrease cell motility, which can lead to prolonged exposure to high light stress and thus increase the risk of photo-damage. At the same time, weakened motility will make it harder for cells to escape predators[4,12].

There is growing concern for how biodiversity loss due to human-induced environmental change will affect the functioning of ecosystems and, in turn, the services ecosystems provide to human beings[19,20]. The influence of elevated $p_{CO_2}$ on the species biodiversity and richness of the phytoplankton assemblages could be profound, through negative effects on some organisms and changes to biogenic habitat[21]. Our study shows, both at physiological and gene-expression levels, that elevated $CO_2$ concentration notable decreases the motility of three typical microalgae after a 5-yr acclimation, which would affect their reproduction and survival, and thus the abundance of microalgae with flagella in aquatic ecosystem. Given that the structure and motility regulation of eukaryotic cilia and flagella are evolutionary conserved[6,22,23], our study reveals the potential effects of aquatic acidification on a wide range of cilia and flagella in eukaryotic organisms, including sperm motility and fertilization[12], cilia-based epithelial fluid flow and the determination of left–right asymmetry[6].

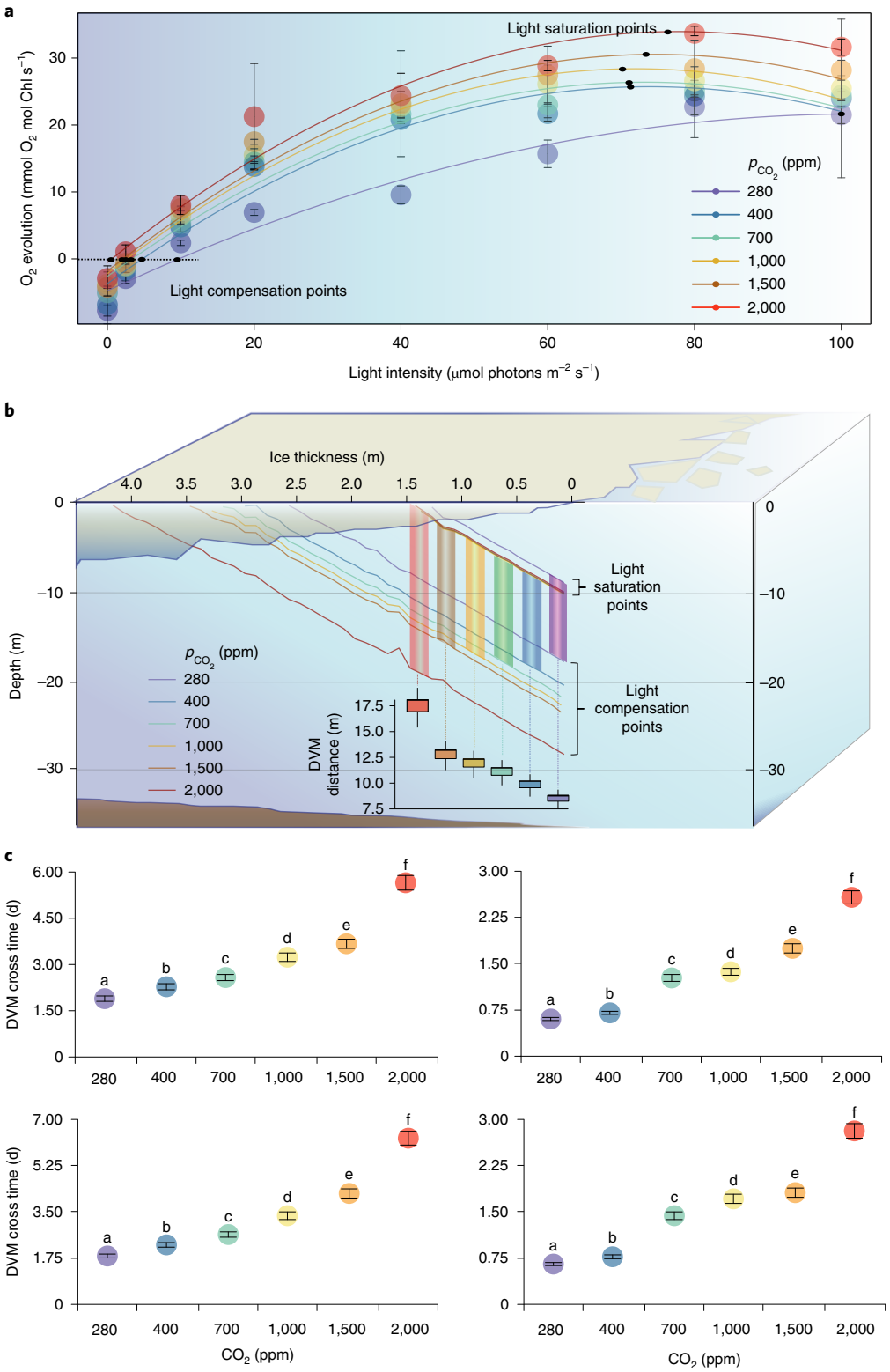


**Fig. 4 | Distribution of *Microglena* sp. and light intensity under melting ice. a**, Photosynthetic light curve of *Microglena* sp. under different $CO_2$ concentrations. Mean ± s.d. values per experimental assay are given ($n = 3$). Chl, chlorophyll. **b**, The incident light distribution in the water under melting ice. Upper and lower horizontal lines represent saturating light intensity and the light compensation point, respectively. *Microglena* sp. lives between the saturated and compensation isophotic lines and moves corresponding to the solar cycle. *Microglena* sp. DVM distance was defined as the vertical distance between the water layer where the light compensation point of algae was located and the water layer where the saturation point was located. **c**, *Microglena* sp. cover the DVM time using the average and instantaneous velocities under positive and negative phototaxis. Upper left, positive phototaxis using average velocity. Upper right, positive phototaxis using instantaneous velocity. Lower left, negative phototaxis using average velocity. Lower right, negative phototaxis using instantaneous velocity. Different letters (a–f) in each panel indicate significant differences ($P < 0.05$) among treatments.

## Online content

Any methods, additional references, Nature Research reporting summaries, source data, extended data, supplementary information, acknowledgements, peer review information; details of author contributions and competing interests; and statements of data and code availability are available at https://doi.org/10.1038/s41558-020-0776-2.

Received: 13 August 2019; Accepted: 9 April 2020;
Published online: 01 June 2020

## References

1. Field, C. B., Behrenfeld, M. J., Randerson, J. T. & Falkowski, P. Primary production of the biosphere: integrating terrestrial and oceanic components. *Science* **281**, 237–240 (1998).
2. Ullah, H., Nagelkerken, I., Goldenberg, S. U. & Fordham, D. A. Climate change could drive marine food web collapse through altered trophic flows and cyanobacterial proliferation. *PLoS Biol.* **16**, e2003446 (2018).
3. Hall, N. S. & Paerl, H. W. Vertical migration patterns of phytoflagellates in relation to light and nutrient availability in a shallow microtidal estuary. *Mar. Ecol. Prog. Ser.* **425**, 7–21 (2015).
4. Stocker, R. & Durham, W. M. Tumbling for stealth? *Science* **325**, 400–402 (2009).
5. Sineshchekov, O. A., Jung, K. H. & Spudich, J. L. Two rhodopsins mediate phototaxis to low- and high-intensity light in *Chlamydomonas reinhardtii*. *Proc. Natl Acad. Sci. USA* **99**, 8689–8694 (2002).
6. Elgeti, J., Winkler, R. G. & Gompper, G. Physics of microswimmers—single particle motion and collective behavior: a review. *Rep. Prog. Phys.* **78**, 1–50 (2015).
7. Caldeira, K. & Wickett, M. E. Anthropogenic carbon and ocean pH. *Nature* **425**, 365 (2003).
8. Flynn, K. J. et al. Changes in pH at the exterior surface of plankton with ocean acidification. *Nat. Clim. Change* **2**, 510–513 (2012).
9. Assmy, P., Fernández-Méndez, M., Duarte, P. & Meyer, A. Leads in Arctic pack ice enable early phytoplankton blooms below snow-covered sea ice. *Sci. Rep.* **7**, 40850 (2017).
10. Kim, H., Spivack, A. J. & Menden-Deuer, S. pH alters the swimming behaviors of the raphidophyte *Heterosigma akashiwo*: implications for bloom formation in an acidified ocean. *Harmful Algae* **26**, 1–11 (2013).
11. Wheeler, G.L. in *Chlamydomonas: Molecular Genetics and Physiology* (Ed. Hippler, M.) 233–255 (Springer, 2017).
12. Waisbord, N. & Guasto, J. S. Peculiar polygonal paths. *Nat. Phys.* **14**, 1157–1162 (2018).
13. Ueki, N. & Wakabayashi, K. Detergent-extracted *Volvox* model exhibits an anterior-posterior gradient in flagellar $Ca^{2+}$ sensitivity. *Proc. Natl Acad. Sci. USA* **115**, E1061–E1068 (2018).
14. Yang, X. L. et al. Effect of melatonin priming on photosynthetic capacity of tomato leaves under low-temperature stress. *Photosynthetica* **56**, 884–892 (2018).
15. Inaba, K. Sperm flagella: comparative and phylogenetic perspectives of protein components. *Mol. Hum. Reprod.* **17**, 524–538 (2011).
16. Lee, J. R. et al. Climate Change drives expansion of Antarctic ice-free habitat. *Nature* **547**, 49–54 (2017).
17. Smetacek, V. & Nicol, S. Polar ocean ecosystems in a changing world. *Nature* **437**, 362–368 (2005).
18. Raymond, J. A. & Morgan-Kiss, R. Multiple ice-binding proteins of probable prokaryotic origin in an Antarctic lake alga, *Chlamydomonas* sp. ice-mdv (Chlorophyceae). *J. Phycol.* **53**, 848–854 (2017).
19. Duffy, J. E., Godwin, C. M. & Cardinale, B. J. Biodiversity effects in the wild are common and as strong as key drivers of productivity. *Nature* **549**, 261 (2017).
20. Hall-Spencer, J. M. & Harvey, B. P. Ocean acidification impacts on coastal ecosystem services due to habitat degradation. *Emerg. Top. Life Sci.* **3**, 197–206 (2019).
21. Sunday, J. M., Fabricius, K. E., Kroeker, K. J. & Anderson, K. M. Ocean acidification can mediate biodiversity shifts by changing biogenic habitat. *Nat. Clim. Change* **7**, 81 (2017).
22. Jeanneret, R., Contino, M. & Polin, M. A brief introduction to the model microswimmer *Chlamydomonas reinhardtii*. *Eur. Phys. J. Spec. Top.* **225**, 2141–2156 (2016).
23. Inaba, K. & Mizuno, K. Sperm dysfunction and ciliopathy. *Reprod. Med. Biol.* **15**, 77–94 (2016).

## Methods

**Cell culture.** *Microglena* sp., *C. reinhardtii* and *D. salina* acquired from Yellow Sea Fisheries Research Institute were used in this study. These three species were semi-continuously cultured in aerated 500-ml conical flasks containing 400 ml of medium (Supplementary Tables 2–4) in a 12/12 h light/dark cycle and at 6, 20 and 20 °C, respectively. *Microglena* sp. was cultured in a series of $CO_2$ treatments (280, 400, 700, 1,000, 1,500 and 2,000 ppm), coded as $M_{280}$, $M_{400}$, $M_{700}$, $M_{1,000}$, $M_{1,500}$ and $M_{2,000}$, respectively. *C. reinhardtii* was cultured in three $CO_2$ treatments (400, 1,000 and 2,000 ppm), coded as $CR_{400}$, $CR_{1,000}$ and $CR_{2,000}$, respectively. *D. salina* was also cultured in three $CO_2$ treatments (400, 1,000 and 2,000 ppm) coded as $DS_{400}$, $DS_{1,000}$ and $DS_{2,000}$, respectively. The ambient $CO_2$ concentration of 400 ppm was designated the control treatment. All cultures (Supplementary Tables 14–16) were conducted in $CO_2$ plant incubators (HP-1000, Ruihua) to maintain the stability of $CO_2$; the variations of $CO_2$ are shown in Supplementary Tables 17–20. The pH in each culture was monitored once every day using a portable pH electrode (6010M, Jenco) to ensure the stability of the pH level during the culture period (Supplementary Tables 17 and 18). All following experiment assays were performed using cells in the light period (6–8 h after the light came on) after the 5-yr acclimation.

**Photosynthesis versus light curve.** For each sample, oxygen production and oxygen uptake were obtained at 6 °C using 4-ml respiration chambers fitted with microprobes, glass-coated stir bars, Clark-type OX-MR oxygen microsensors and a PA 2000 picoammeter. Data were logged using MicOx 2.6 data acquisition software (Microrespiration system, Unisense). Oxygen microsensors were polarized continuously for >24 h before use. Oxygen production and oxygen uptake ratio were recorded at different light intensities using light-emitting diodes (LEDs) and then fitted to the relationships described by Platt et al.[24] (Supplementary Table 21). The intersection point between the photosynthetic oxygen evolution curve and the *x* axis is the light compensation point; the point when the photosynthetic oxygen evolution reaches its maximum value is the light saturation point.

**Chlorophyll determination.** Fresh algal cells collected in a 2-ml centrifuge tube from 2 ml of cultivated broth by centrifuge were disrupted in an ultrasonic bath (KQ3200DA, Kunshan) in ice bath for 45 min and extracted with 2 ml of 95% ethanol overnight in 4 °C. The extractant was centrifuged at 3,000*g* for 5 min (ref. [25]). The chlorophyll (Chl) content was determined spectrophotometrically as follows:

$Chl = 5.24A_{664.2} + 22.24A_{648.6}$, where $A_{664.2}$ and $A_{648.6}$ represent absorbance of the methanol extracts at 664.2 and 648.6 nm, respectively[26].

**Light intensity for positive and negative phototaxis.** Phototaxis is the biological tendency to move under light stimulation. Positive phototaxis occurs when algae sense light through the eyespot and move toward it using their motor organs. Negative phototaxis is a reaction of algae to sense light through the eyespot and move away from it using their motor organs. Compared with *C. reinhardtii*, *Microglena* sp. had a very low light compensation point (4.8 μmol photons $m^{-2}$ $s^{-1}$) and saturation point (73.82 μmol photons $m^{-2}$ $s^{-1}$), about 10% that of *C. reinhardtii* under normal conditions (Fig. 4a). Light density distribution with variations in incident irradiance were measured during the positive/negative phototaxis assays of *Microglena* sp., *C. reinhardtii* and *D. salina* (Supplementary Figs. 12 and 13). Consequently, irradiances of 2 μmol photons $m^{-2}$ $s^{-1}$ and 200 μmol photons $m^{-2}$ $s^{-1}$ were selected as the positive phototaxis-inducing light and negative phototaxis-inducing light, respectively. For *C. reinhardtii* and *D. salina*, the positive phototaxis-inducing light was the same as that inducing *Microglena* sp. and negative phototaxis-inducing light was 800 μmol photons $m^{-2}$ $s^{-1}$ (refs. [27–29]).

**Vertical cell motion.** Cells were washed with pre-acidified experimental solution with different $p_{CO_2}$ and kept under red light for >50 min before the assays[30]. In all the experiments involving light induction, we use a customized LED with multiple lamp beads, which can emit parallel light of wavelengths of 400–700 nm and with the light intensity adjustable in the range 0–2,000 μmol photons $m^{-2}$ $s^{-1}$. For vertical laboratory microscale experiments, the acrylic channel used had an inner diameter of 4.4 cm and a height of 11 cm (Supplementary Figs. 8a and 10a). To maintain the stability of the acrylic channel, in the outdoor experiment, we extended the length of the acrylic channel to 40 cm and used only the top 11 cm during mesoscale experiments (Supplementary Fig. 9a). For the positive phototaxis assays, 15 ml of cell suspensions (~$2.4\times10^6$ cells $ml^{-1}$) were placed into the bottom of acrylic channels by a pipette, illuminated with an LED (white/blue, ~2 μmol photons $m^{-2}$ $s^{-1}$) from immediately above for 20 min and sampled every centimetre (Supplementary Fig. 10a). For the negative phototaxis assays, 15 ml of cell suspensions (~$2.4\times10^6$ cells $ml^{-1}$) were placed into the top of the acrylic channels by a pipette, illuminated with an LED (white/blue, ~200 μmol photons $m^{-2}$ $s^{-1}$/~800 μmol photons $m^{-2}$ $s^{-1}$) from immediately above for 20 min and sampled every centimetre (Supplementary Fig. 10a). The positive phototaxis assay treatment was used to keep cells at the top of the vessel during the negative phototaxis assays. To calculate the cell velocity, we chose the average distance from the sampling point to the loading point (as a point without volume) as the distance of the cells had moved at each sampling point. The distance moved was set to 0.5, 1.5, 2.5, 3.5, 4.5, 5.5, 6.5, 7.5, 8.5 and 9.5 cm corresponding to samples from one to ten, respectively. The average velocity was calculated as follows:

$$\text{Velocity} = (C_1V_1\times S_1 + C_2\times V_2\times S_2 + \ldots\ \ldots\ + C_{10}\times V_{10}\times S_{10}) /t/(C_1\times V_1 + C_2\times V_2 + \ldots\ \ldots\ + C_{10}\times V_{10}) \quad (1)$$

where *C* is cell concentration, *V* is sample volume, *S* is distance moved and *t* is move time.

**Horizontal cell motion.** Cells were washed with a pre-acidified experimental solution with different $CO_2$ concentrations and kept under red light for >50 min before the assays. For horizontal laboratory microscale experiments, the acrylic channel was oblong with a square cross-section, each side being 4 cm and channels evenly divided into 11 parts with a width of 1 cm each (Supplementary Figs. 8b and 10b). As for the vertical cell motion study, to maintain the stability of the acrylic channel in the outdoor experiment, we extended the length of the acrylic channel to 40 cm and used 11 cm on one end during mesoscale experiments (Supplementary Fig. 9d). For the positive phototaxis assays, 15 ml of cell suspensions (~$2.4\times10^6$ cells $ml^{-1}$) were placed into one side of the acrylic channels, matching acrylic cards were inserted to separate the cell suspensions after illuminating with an LED (white, ~2 μmol photons $m^{-2}$ $s^{-1}$) from the opposite side for 20 min, and then samples were collected every sample point (Supplementary Fig. 10b). For the negative phototaxis assays, 15 ml of cell suspensions (~$2.4\times10^6$ cells $ml^{-1}$) were placed into one side of acrylic channels, illuminated with an LED (white, ~200 μmol photons $m^{-2}$ $s^{-1}$/~800 μmol photons $m^{-2}$ $s^{-1}$) from the side for 20 min, and then samples were collected every sample point (Supplementary Fig. 10b). To calculate the cell velocity, we chose the average distance from the sampling point to the loading point (as a point without volume) as the distance of the cells at each sampling point. The distance moved was set to 0.5, 1.5, 2.5, 3.5, 4.5, 5.5, 6.5, 7.5, 8.5 and 9.5 cm corresponding to samples from one to ten, respectively. The average velocity was calculated as in equation (1).

**Field experiment.** To further study the effect of ocean acidification on algal motion in a more natural ocean setting, we investigated the average velocity of *Microglena* sp. induced by sunlight in a calm bay (Supplementary Fig. 9). The horizontal and vertical sampling methods were consistent with the laboratory experiment but the channel length was increased to 40 cm to ensure the stability of the equipment in seawater. The vertical channels were divided into two parts by rubber plug, the front part being 11 cm, the back part 29 cm; the latter part was injected with natural seawater to keep the tank stable. The horizontal channels were divided into two sections by acrylic spacers, the first section being 11 cm, the second section 29 cm; the latter section was injected with natural seawater to keep the tank stable. In our experiment, we only used the front end 11 cm.

**Flagellum shedding and regeneration.** *Microglena* sp. was cultured to the exponential growth stage at the different pH values and then aeration was stopped. We used a Nikon Eclipse 80i microscope (Carl Zeiss) to look at the flagella and calculated the percentage of cells without flagella compared to total cells. pH-Shocked cells were obtained by rapidly adding a large amount of culture medium saturated with $CO_2$ to the culture medium containing motile cells, centrifugation was conducted, and medium with different acidification gradients was added. The proportion of flagellar regeneration was calculated by recording the motility of the cells.

**Transcriptome.** To explore the mechanism by which *Microglena* sp. responds to ocean acidification, on year 5 of the long-term experiment, the cultures of *Microglena* sp. $M_{400}$ and $M_{1,000}$ were selected, centrifuged at 6 °C frozen in liquid nitrogen and stored at −80 °C for subsequent transcriptomic analysis (with three biological replicates for each sample). To avoid circadian bias, our sampling time was 6 h after illumination, that is 14:00 h for all samples.

**RT–PCR.** RNA isolated from *Microglena* sp. ($M_{400}$, $M_{1,000}$ and $M_{2,000}$) was treated with DNase I and then reverse-transcribed to complementary DNA using random hexamers. PCR was then performed using cDNA templates and primers specific for *Microglena* sp. genes MigICE16000, MigICE12547, MigICE10361, MigICE11569, MigICE4581, MigICE14893, MigICE8486, MigICE16283, MigICE4131, MigICE16837, MigICE5195, MigICE9498, MigICE14891 and MigICE16200. Control PCR reactions were performed using chromosomal DNA templates and the same primer sets under the same PCR conditions. To avoid circadian bias, our sampling time was 6 h after illumination, that is 14:00 h for all samples.

**Calcium ions flux measurements.** The net flux of $Ca^{2+}$ between intracellular and extracellular was measured non-invasively using the scanning ion-selective electrode technique (SIET system, BIO-001A, Younger USA Sci. & Tech., Applicable Electronics and Science Wares). The measurements of the $Ca^{2+}$ flux was performed as described by Sun et al. with some modifications[31]. Cells

of *Microglena* sp. were settled on the centre of a cover slip pre-treated wtih poly-L-lysine and then placed in 4 ml of measuring solution (0.2 mM $CaCl_2$, 360 mM NaCl, 2.0 mM $NaHCO_3$, 8.0 mM KCl, 0.1 mM $Na_2SO_4$, 0.05 mM $H_3BO_3$, 0.5 mM $NH_4NO_3$, 2.0 mM Tris). Solution was pre-acidified at the corresponding $p_{CO_2}$ before $Ca^{2+}$ flux measurements. Three-dimensional ionic flux signals were continuously recorded for 5 min and plotted with MageFlux software that was developed by Xu Yue (http://xuyue.net/mageflux).

***Microglena* sp. distribution and irradiance at different depths under melting ice.** *Microglena* sp. live in the seawater beneath sea ice. Light intensity at the boundary of ice and water increases with external light intensity. When the light intensity exceeds the *Microglena* sp. saturation point, the algae move downward to escape the strong light. When the light is lower than compensation point, the algae move upward to find the appropriate light intensity. We define the distance between compensation point and saturation point as distance of DVM. During a light cycle, *Microglena* sp. move up and down in seawater within the DVM. Light levels, which were attenuated by sea ice, were obtained from the formula $T = e^{-kb}$ where $T$ is the extinction coefficient, $e$ is the Napierian base, $k$ a constant and $b$ the optical path[32]. The intensity of light decreases gradually with the thickness of sea ice due to the attenuation effect of sea ice on light. Light levels in seawater were obtained using data that we measured in the North Yellow Sea in October. Sea ice used in this experiment was artificially made from cold storage. After the natural seawater was filtered, the salinity was adjusted to five practical salinity units with deionized water and the temperature was lowered to −15 °C to obtain sea ice of different thicknesses.

**Instantaneous velocity.** Measurement of cell instantaneous velocity was based on the modified method of previous studies[30,33] using particle image velocimetry (PIV) (Stereo-PIV, TSI)[30,33]. The container (side length 10 cm, opening above) was illuminated from one side by a laser sheet with a wavelength of 532 nm (the light that records the movement of cells). Phototactic responses of the cells were observed when the container was illuminated by LED (SRZ-BLTO9W-01, GeShuo) from the top or side. The light intensity was 2 and 200 μmol photons $m^{-2} s^{-1}$ at the top and side surface of the suspension. The illumination was slightly reduced as the depth within the vessel increased. To avoid the slightly non-uniform illumination effect, the brightness of the image at the same depth for the PIV analysis was measured. For *C. reinhardtii* and *D. salina*, the positive phototaxis-inducing light was 2 μmol photons $m^{-2} s^{-1}$ and negative phototaxis-inducing light was 800 μmol photons $m^{-2} s^{-1}$.

The instantaneous velocity was calculated as follows:

$$\text{Velocity} = S/t \quad (2)$$

where $S$ is displacement and $t$ is move time = 1 s.

**Statistical analyses.** Each result shown is the mean of at least three biological replicates.

Statistical analyses were performed using SPSS v.22 for Windows (SPSS). Since some datasets did not conform to the normal distribution, the Kruskal–Wallis test was used to analyse the effects of $CO_2$. Variance among treatments was tested using the Kruskal–Wallis test followed by Dunn's post-hoc test; except for the comparison between two sets of data in Supplementary Tables 1–12, which were tested using the Kruskal–Wallis test followed by Tamhane's post-hoc test. The significance level was $P < 0.05$ for all tests.

**Reporting Summary.** Further information on research design is available in the Nature Research Reporting Summary linked to this article.

## Data availability

The data that support the findings of this study are available from the corresponding author upon reasonable request. Source Data for Figs. 1–4 and Extended Data Figs. 1–4 are provided with the paper.

## References


24. Platt., T., Gallagos., C. C. & Hamson., W. G. Photoinhibition of photosynthesis in natural assemblages of marine phytoplankton. *J. Mar. Res.* **38**, 687–701 (1980).
25. Li, Y., Horsman, M., Wang, B., Wu, N. & Lan, C. Q. Effects of nitrogen sources on cell growth and lipid accumulation of green alga *Neochloris oleoabundans*. *Appl. Microbiol. Biotechnol.* **81**, 629–636 (2008).
26. Lichtenthaler, H. K. Chlorophylls and carotenoids: pigments of photosynthetic biomembranes. *Methods Enzymol.* **148**, 350–382 (1987).
27. Sültemeyer, D. F., Klug, K. & Fock, H. P. Effect of photon fluence rate on oxygen evolution and uptake by *Chlamydomonas reinhardtii* suspensions grown in ambient and $CO_2$-enriched air. *Plant Physiol.* **81**, 372–375 (1986).
28. Rühle, T., Hemschemeier, A., Melis, A. & Happe, T. A novel screening protocol for the isolation of hydrogen producing *Chlamydomonas reinhardtii* strains. *BMC Plant Biol.* **8**, 107 (2008).
29. Sültemeyer, D. F., Klock, G., Kreuzberg, K. & Fock, H. P. Photosynthesis and apparent affinity for dissolved inorganic carbon by cells and chloroplasts of *Chlamydomonas reinhardtii* grown at high and low $CO_2$ concentrations. *Planta* **176**, 256–260 (1988).
30. Ueki, N., Ide, T., Mochiji, S., Kobayashi, Y. & Tokutsu, R. Eyespot-dependent determination of the phototactic sign in *Chlamydomonas reinhardtii*. *Proc. Natl Acad. Sci. USA* **113**, 5299–5304 (2016).
31. Sun, J. et al. $H_2O_2$ and cytosolic $Ca^{2+}$ signals triggered by the PM $H^+$-coupled transport system mediate $K^+/Na^+$ homeostasis in NaCl-stressed *Populus euphratica* cells. *Plant Cell Environ.* **33**, 943–958 (2010).
32. Perovich, D. K. & Grenfell, T. C. Laboratory studies of the optical properties of young sea ice. *J. Glaciol.* **27**, 331–346 (1981).
33. Massa, T., Genina, A., Shavitc, U., Grinsteind, M. & Tchernov, D. Flow enhances photosynthesis in marine benthic autotrophs by increasing the efflux of oxygen from the organism to the water. *Proc. Natl Acad. Sci. USA* **107**, 2527–2531 (2010).


## Acknowledgements

This work was supported by the national key research and development programme of China (grant no. 2018YFD0900703); Marine S&T Fund of Shandong Province for Pilot National Laboratory for Marine Science and Technology (Qingdao) (grant no. 2018SDKJ0406-3); Major Scientific and Technological Innovation Project of Shandong Provincial Key Research and Development Program (grant no. 2019JZZY020706); Central Public-interest Scientific Institution Basal Research Fund, CAFS (grant no. 2020TD27); China Agriculture Research System (grant no. CARS-50); Financial Fund of the Ministry of Agriculture and Rural Affairs, P.R. China (grant no. NFZX2018); Taishan Scholars Funding and Talent Projects of Distinguished Scientific Scholars in Agriculture.

## Author contributions

N.H.Y. designed the project. Y.T.W., D.X., X.W.Z. and W.T.H. performed the research. F.X., N.H.Y. and Y.T.W. analysed the data. Y.T.W., N.H.Y., G. G. and F.X. wrote the first draft. All authors contributed to interpreting the data and writing the manuscript.

## Competing interests

The authors declare no competing interests.

## Additional information

**Extended data** is available for this paper at https://doi.org/10.1038/s41558-020-0776-2.

**Supplementary information** is available for this paper at https://doi.org/10.1038/s41558-020-0776-2.

**Correspondence and requests for materials** should be addressed to N.Y.

**Peer review information** *Nature Climate Change* thanks Jolanda Verspagen and the other, anonymous, reviewer(s) for their contribution to the peer review of this work.

**Reprints and permissions information** is available at www.nature.com/reprints.

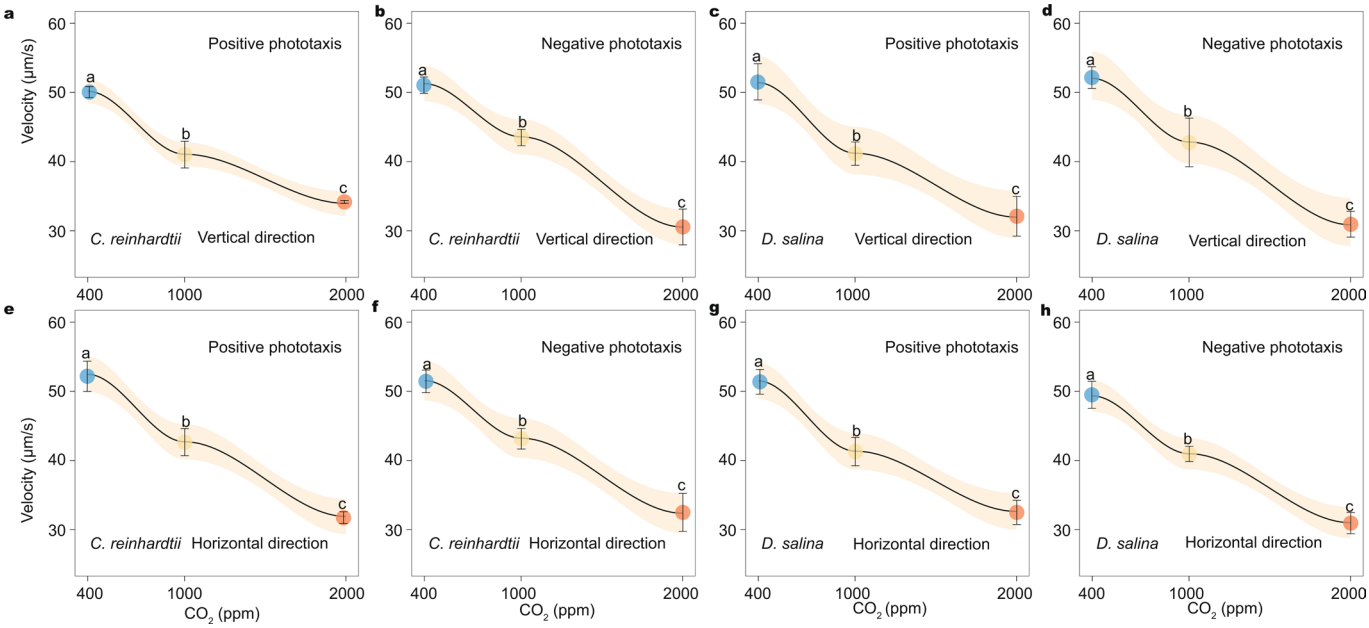


**Extended Data Fig. 1 | Average velocity of *C. reinhardtii* and *D. salina*.** **a**, *C. reinhardtii* positive phototaxis induced by white light in the vertical direction. **b**, *C. reinhardtii* negative phototaxis induced by white light in the vertical direction. **c**, *D. salina* positive phototaxis induced by white light in the vertical direction. **d**, *D. salina* negative phototaxis induced by white light in the vertical direction. **e**, *C. reinhardtii* positive phototaxis induced by white light in the horizontal direction. **f**, *C. reinhardtii* negative phototaxis induced by white light in the horizontal direction. **g**, *D. salina* positive phototaxis induced by white light in the horizontal direction. **h**, *D. salina* negative phototaxis induced by white light in the horizontal direction. Mean ± SD values per experimental assay are given (n = 3).

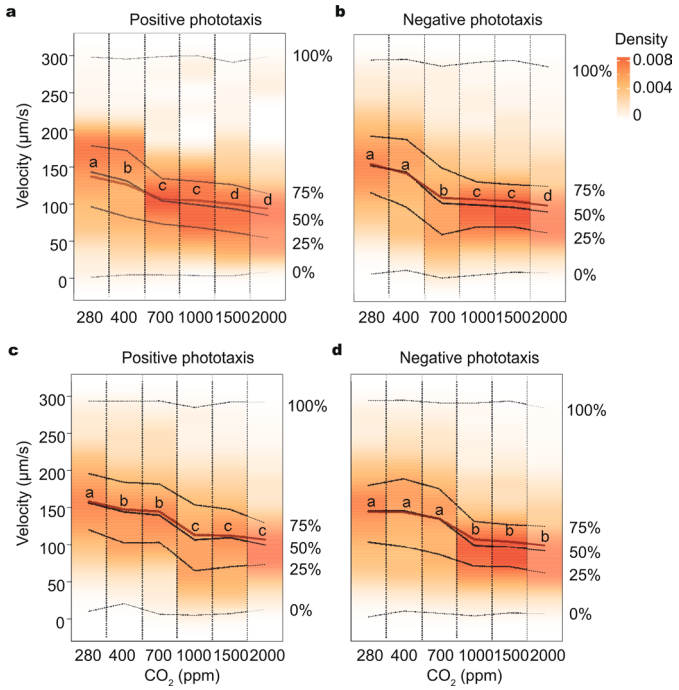


**Extended Data Fig. 2 | Instantaneous velocity of *Microglena* sp. a**, Positive phototaxis induced by white light in the vertical direction. **b**, Negative phototaxis induced by white light in the vertical direction. **c**, Positive phototaxis induced by white light in the horizontal direction. d, Negative phototaxis induced by white light in the horizontal direction. The colour scale indicates the density of the cell distribution under various velocities. A total of 300 data points was collected for each experimental treatment. The five dotted lines correspond to 0%, 25%, 50%, 75%, 100%, respectively. Each dotted line represents the cumulative ratio, the number of cells below the dotted line as a percentage of the total number of cells. The solid line represents the average velocity and letters indicate significant differences between $CO_2$ treatments ($P < 0.05$). Different letters in superscript indicate significant differences ($P < 0.05$) among treatments (Kruskal Wallis test followed by Dunn's post-hoc test).

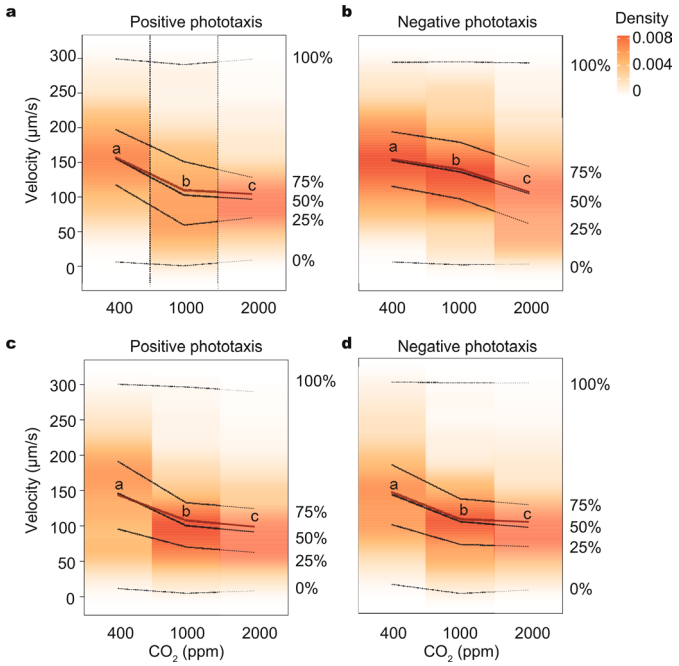


**Extended Data Fig. 3 | Instantaneous velocity of *C. reinhardtii* and *D. salina* in the vertical direction. a**, *C. reinhardtii* positive phototaxis induced by white light. **b**, *C. reinhardtii* negative phototaxis induced by white light. **c**, *D. salina* positive phototaxis induced by white light. **d**, *D. salina* negative phototaxis induced by white light. The colour scale indicates the density of the cell distribution under various velocities. A total of 300 data points was collected for each experimental treatment. The five dotted lines correspond to 0%, 25%, 50%, 75%, 100%, respectively. Each dotted line represents the cumulative ratio, the number of cells below the dotted line as a percentage of the total number of cells. The solid line represents the average velocity and letters indicate significant differences between $CO_2$ treatments ($P < 0.05$). Different letters in superscript indicate significant differences ($P < 0.05$) among treatments (Kruskal Wallis test followed by Dunn's post-hoc test).

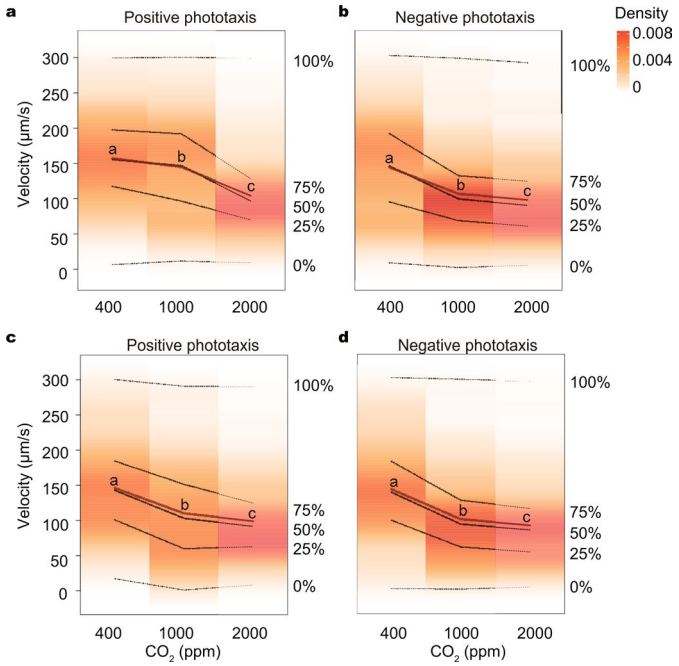


**Extended Data Fig. 4 | Instantaneous velocity of *C. reinhardtii* and *D. salina* in the horizontal direction. a**, *C. reinhardtii* positive phototaxis induced by white light. **b**, *C. reinhardtii* negative phototaxis induced by white light. **c**, *D. salina* positive phototaxis induced by white light. **d**, *D. salina* negative phototaxis induced by white light. The colour scale indicates the density of the cell distribution under various velocities. A total of 300 data points was collected for each experimental treatment. The five dotted lines correspond to 0%, 25%, 50%, 75%, 100%, respectively. Each dotted line represents the cumulative ratio, the number of cells below the dotted line as a percentage of the total number of cells. The solid line represents the average velocity and letters indicate significant differences between $CO_2$ treatments ($P < 0.05$). Different letters in superscript indicate significant differences ($P < 0.05$) among treatments (Kruskal Wallis test followed by Dunn's post-hoc test).

nature research

Corresponding author(s): Naihao Ye

Last updated by author(s): Mar 18, 2020

# Reporting Summary

Nature Research wishes to improve the reproducibility of the work that we publish. This form provides structure for consistency and transparency in reporting. For further information on Nature Research policies, see Authors & Referees and the Editorial Policy Checklist.

## Statistics

For all statistical analyses, confirm that the following items are present in the figure legend, table legend, main text, or Methods section.

| n/a | Confirmed | |
|---|---|---|
| ☐ | ☒ | The exact sample size (*n*) for each experimental group/condition, given as a discrete number and unit of measurement |
| ☐ | ☒ | A statement on whether measurements were taken from distinct samples or whether the same sample was measured repeatedly |
| ☐ | ☒ | The statistical test(s) used AND whether they are one- or two-sided<br>*Only common tests should be described solely by name; describe more complex techniques in the Methods section.* |
| ☒ | ☐ | A description of all covariates tested |
| ☐ | ☒ | A description of any assumptions or corrections, such as tests of normality and adjustment for multiple comparisons |
| ☐ | ☒ | A full description of the statistical parameters including central tendency (e.g. means) or other basic estimates (e.g. regression coefficient) AND variation (e.g. standard deviation) or associated estimates of uncertainty (e.g. confidence intervals) |
| ☐ | ☒ | For null hypothesis testing, the test statistic (e.g. *F*, *t*, *r*) with confidence intervals, effect sizes, degrees of freedom and *P* value noted<br>*Give P values as exact values whenever suitable.* |
| ☒ | ☐ | For Bayesian analysis, information on the choice of priors and Markov chain Monte Carlo settings |
| ☒ | ☐ | For hierarchical and complex designs, identification of the appropriate level for tests and full reporting of outcomes |
| ☒ | ☐ | Estimates of effect sizes (e.g. Cohen's *d*, Pearson's *r*), indicating how they were calculated |

*Our web collection on statistics for biologists contains articles on many of the points above.*

## Software and code

Policy information about availability of computer code

| | |
|---|---|
| Data collection | Calcium ions flurescence data were collected using Leica LAS AF software. Chlorophyll flurescence data were collected using Walz imagingWin software. Instantaneous velocity data were collected INSIGHT™ 4G software. |
| Data analysis | SPSS v.22, R 3.5.1 |

For manuscripts utilizing custom algorithms or software that are central to the research but not yet described in published literature, software must be made available to editors/reviewers. We strongly encourage code deposition in a community repository (e.g. GitHub). See the Nature Research guidelines for submitting code & software for further information.

## Data

Policy information about availability of data

All manuscripts must include a data availability statement. This statement should provide the following information, where applicable:

- Accession codes, unique identifiers, or web links for publicly available datasets
- A list of figures that have associated raw data
- A description of any restrictions on data availability

The data that support the findings of this study are available from the corresponding author upon reasonable request.

# Field-specific reporting

Please select the one below that is the best fit for your research. If you are not sure, read the appropriate sections before making your selection.

☐ Life sciences ☐ Behavioural & social sciences ☒ Ecological, evolutionary & environmental sciences

# Ecological, evolutionary & environmental sciences study design

All studies must disclose on these points even when the disclosure is negative.

| | |
|---|---|
| Study description | Using a six-level, CO2 gradient experiment, we investigated the changes in the velocity of Microglena sp. under laboratory microscale. Field mesoscale experiments were investigated using three-level CO2 gradient. Changes in the expression of motility-related genes was investigated. The effects of three-level CO2 gradient experiment on Dunaliella salina and Chlamydomonas reinhardtii velocity have also been done. See manuscript for full details. |
| Research sample | Microglena sp., Chlamydomonas reinhardtii and Dunaliella salina were used in this study. These three species were semi-continuously cultured in aerated 500 ml conical flasks containing 400 ml of medium in a 12-h/12-h light/dark cycle and at 6 °C, 20 °C, 20 °C, respectively. All following experiment assays were performed using cells in the light period (6~8 h after the light came on) after the five-year acclimation. |
| Sampling strategy | Microglena sp., Chlamydomonas reinhardtii and Dunaliella salina were measured for motility in the light period (6~8 h after the light came on) after the five-year acclimation. Motility-related genes expression of Microglena was 6 hours after illumination. |
| Data collection | Y.T.W., D.X., X.W.Z. and W.T.H collected the data. |
| Timing and spatial scale | All data of Microglena sp., Chlamydomonas reinhardtii and Dunaliella salina were done after five-year acclimation expect for SNP data which lasting from the first year to the fifth year . |
| Data exclusions | No data has been excluded. |
| Reproducibility | Before the formal experiment, we did many pre-experiments to make sure that our operation is correct and the experiments are repeatable. In addition, three algae species were used and short-term and long-term experiments were conducted, which output similar results. |
| Randomization | Randomised sampling strategies were used in all sampling , with replicates analysed in random order. |
| Blinding | Complete blinding of data analysis was used. |

Did the study involve field work? ☒ Yes ☐ No

## Field work, collection and transport

| | |
|---|---|
| Field conditions | Temperatures were approx. 5.0 - 7.0°C. Daily light cycle was 11:13 h light:dark. |
| Location | The experiment was carried out in the sea , approx. 1 km offshore ,<br>Qingdao (36.05° N, 120.36° E). |
| Access and import/export | The site where field experiments were conducted is a public area and open to everyone. |
| Disturbance | The field experiments were conducted in an enclosure system, which minimized the disturbance to local ecosystem. |

# Reporting for specific materials, systems and methods

We require information from authors about some types of materials, experimental systems and methods used in many studies. Here, indicate whether each material, system or method listed is relevant to your study. If you are not sure if a list item applies to your research, read the appropriate section before selecting a response.

### Materials & experimental systems

| n/a | Involved in the study |
|---|---|
| ☒ | ☐ Antibodies |
| ☐ | ☒ Eukaryotic cell lines |
| ☒ | ☐ Palaeontology |
| ☒ | ☐ Animals and other organisms |
| ☒ | ☐ Human research participants |
| ☒ | ☐ Clinical data |

### Methods

| n/a | Involved in the study |
|---|---|
| ☒ | ☐ ChIP-seq |
| ☒ | ☐ Flow cytometry |
| ☒ | ☐ MRI-based neuroimaging |

## Eukaryotic cell lines

Policy information about cell lines

| | |
|---|---|
| Cell line source(s) | Microglena sp. was obtained from the Algae Culture Collection at the Institute of Yellow Sea Fisheries Research Institute (YSFRI). Chlamydomonas reinhardtii was obtained from Freshwater Algae Culture Collection at the Institute of Hydrobiology, Chinese Academy of Sciences. Dunaliella salina was obtained from the National Institute for Environmental Studies (NIES Collection, Tsukuba, JAPAN). |
| Authentication | We identified atpB, psaA, psaB, psbC and rbcL genes and classified the polar marine alga into the genus of Microglen (Demchenko, E., Mikhailyuk, T., W. Coleman, A. & Pröschold, T. Generic and species concepts in Microglena (previously the Chlamydomonas monadina group) revised using an integrative approach. European Journal of Phycology - EUR J PHYCOL 47, 264-290, doi:10.1080/09670262.2012.678388 (2012).). Chlamydomonas reinhardtii is numbered Chlamydomonas reinhardtii FACHB-2217 in FACHB. Dunaliella salina is numbered Dunaliella salina NIES-2257 in NIES. |
| Mycoplasma contamination | Using transcriptome and genome data, we found that the results of Mycoplasma contamination were negative. |
| Commonly misidentified lines (See ICLAC register) | There is no commonly misidentified cell lines used in the study. |